

RESEARCH ARTICLE

Cytotoxic, anti-inflammatory, antioxidant, and anti-glyoxalase-I evaluation of chelating substances: In silico and in vitro study

MohammedBashar Al-Qazzan^{1,2*}, Qosay Al-Balas³, Belal Alnajjar¹, Violet Kasabri^{4*}, Yusuf Al-Hiari⁴, Aref Zayed^{1,3}, Rema AlKhateeb⁴, Mohammed Al-Akeedi⁵

1 Department of Pharmaceutical Sciences, Faculty of Pharmacy, Al-Ahliyya Amman University, Amman, Jordan, **2** College of Pharmacy, University of Bilad Alrafidain, Diyala, Iraq, **3** Department of Medicinal Chemistry and Pharmacognosy, Faculty of Pharmacy, Jordan University of Science & Technology, Irbid, Jordan, **4** School of Pharmacy, University of Jordan, Amman, Jordan, **5** College of Pharmacy, The University of Mashreq, Baghdad, Iraq

* alanim050@gmail.com (MBA); violetk70@gmail.com (VK)



Abstract

Introduction

Glyoxalase I is a crucial target in cancer treatment due to its involvement in detoxifying methylglyoxal. Suppressing the activity of Glyoxalase I has great potential for disrupting the pathways that allow cancer cells to survive, creating a new route for cancer treatment.

Methodology

This study aims to investigate several substances as inhibitors of glyoxalase-I. After demonstrating their efficacy, additional inquiry will concentrate on assessing their cytotoxic and anti-inflammatory capabilities, yielding significant insights for prospective medicinal uses. The selection of these chemicals as potential Glyoxalase I inhibitors was based on their ability to bind metals, in crucial enzymes. These compounds consist of catechol, dihydroxy, trihydroxy benzene, and functional groups such hydroxamic acid, sulfur, carboxylic acid, amide, and 3-hydroxy-4-pyridone with the aim to suppress Glyoxalase I *in vitro*. Docking protocol was employed to examine the binding interactions with the active site. These auspicious compounds have been subjected to cytotoxicity assay testing employing Sulforhodamine B in eleven distinct cell lines, as well as anti-inflammatory and antioxidant evaluations.

Results

Glyoxalase I inhibition revealed that 4-hydroxy-estradiol exhibited the highest efficacy with an IC_{50} value of 0.226 μ M. Trichostatin A demonstrated a significant anti-proliferation effect in colorectal cancer cells (CACO2, HCT116, SW620, HT29) with

OPEN ACCESS

Citation: Al-Qazzan M, Al-Balas Q, Alnajjar B, Kasabri V, Al-Hiari Y, Zayed A, et al. (2025) Cytotoxic, anti-inflammatory, antioxidant, and anti-glyoxalase-I evaluation of chelating substances: In silico and in vitro study. PLoS One 20(10): e0333405. <https://doi.org/10.1371/journal.pone.0333405>

Editor: Afzal Basha Shaik, Vignan Pharmacy College, INDIA

Received: February 24, 2025

Accepted: September 14, 2025

Published: October 15, 2025

Peer Review History: PLOS recognizes the benefits of transparency in the peer review process; therefore, we enable the publication of all of the content of peer review and author responses alongside final, published articles. The editorial history of this article is available here: <https://doi.org/10.1371/journal.pone.0333405>

Copyright: © 2025 Al-Qazzan et al. This is an open access article distributed under the terms of the [Creative Commons Attribution License](#), which permits unrestricted use, distribution,

and reproduction in any medium, provided the original author and source are credited.

Data availability statement: All relevant data are within the manuscript and its [Supporting information](#) files.

Funding: The author(s) received no specific funding for this work.

Competing interests: The authors have declared that no competing interests exist.

IC_{50} values ranging from 14.0 μ M to 27.0 μ M. Furthermore, it exhibited substantial decreases in viability, ranging from 1.4 μ M to 14.7 μ M, in cancer cell cultures of skin (A375), lung (A549), prostate (PC3), breast (MCF7 and T47D), and cervical (HeLa). Except for 4-hydroxyestradiol, the other phytochemicals demonstrated considerable selectivity in reducing the viability of cancer cells in monolayers of colorectal, cervical, mammary, lung, and skin tissues. In comparison to indomethacin and vitamin C, all of the studied natural compounds exhibited excellent anti-inflammatory properties in LPS-primed RAW 264.7 murine macrophages and had moderate antioxidant abilities comparable to ascorbic acid, with IC_{50} values from 26.0 μ M to 99.0 μ M.

Conclusion

Further assessment of molecular action mechanisms and structural betterments/enhancements and/or derivatization of promising potent agents with antiglyoxylase – antiinflammation duality along with differential cytotoxicity and reductive capacities are advisably warranted with appropriately matched downstream *in vivo* validation modalities.

Introduction

Cancer is a condition characterized by uncontrolled cellular proliferation that occurs in the human body due to the accumulation of genetic and epigenetic changes in normal cells [1]. Cancer is a significant global health issue, despite ongoing endeavors to address it [2]. Hence, it is crucial to discover innovative pharmaceuticals and study cancer behavior in order to uncover new targets for medication development. The potential of selectively inhibiting Glyoxalase I (Glo-I); as a therapeutic target, has been identified with promising outcomes [3–5]. The glyoxalase system carries out a detoxification function within living cells. It participates in the catalysis of GSH-dependent reactions by converting oxoaldehydes, such as methylglyoxal, into D-lactic acid, as illustrated in [Fig 1](#) [6–8]. Methylglyoxal is a noxious byproduct of regular metabolism, generated during the glycolysis process [9]. The glyoxalase system consists of two enzymes, glyoxalase I (Glo-I) and glyoxalase II (Glo-II), along with some amount of glutathione (GSH) that acts as a catalyst. It has been suggested that inhibiting the glyoxalase pathway, particularly Glo-I, in cancer cells leads to the accumulation of toxic methylglyoxal, which in turn induces self-destruction of the cancer cells [10]. Advanced Glycation End Products (AGEs) play a major role in the development of diabetes, cardiovascular disease (CVD), and cancer. Glo-I is heavily involved in the body's defenses against glycation [11]. Inhibiting the Glo system has shown great promise as a potential therapy for treating and preventing tumors [12–14]. Increased levels of Glo-I, as a biomarker for tumors, have been linked to multidrug resistance in cancer chemotherapy [5,15,16]. Additionally, novel Glo inhibitors with a “zinc-binding feature” have been reported to possess anticancer properties, similar to anticancer metallo-drugs that inhibit cell proliferation through mitochondrial intrinsic apoptosis

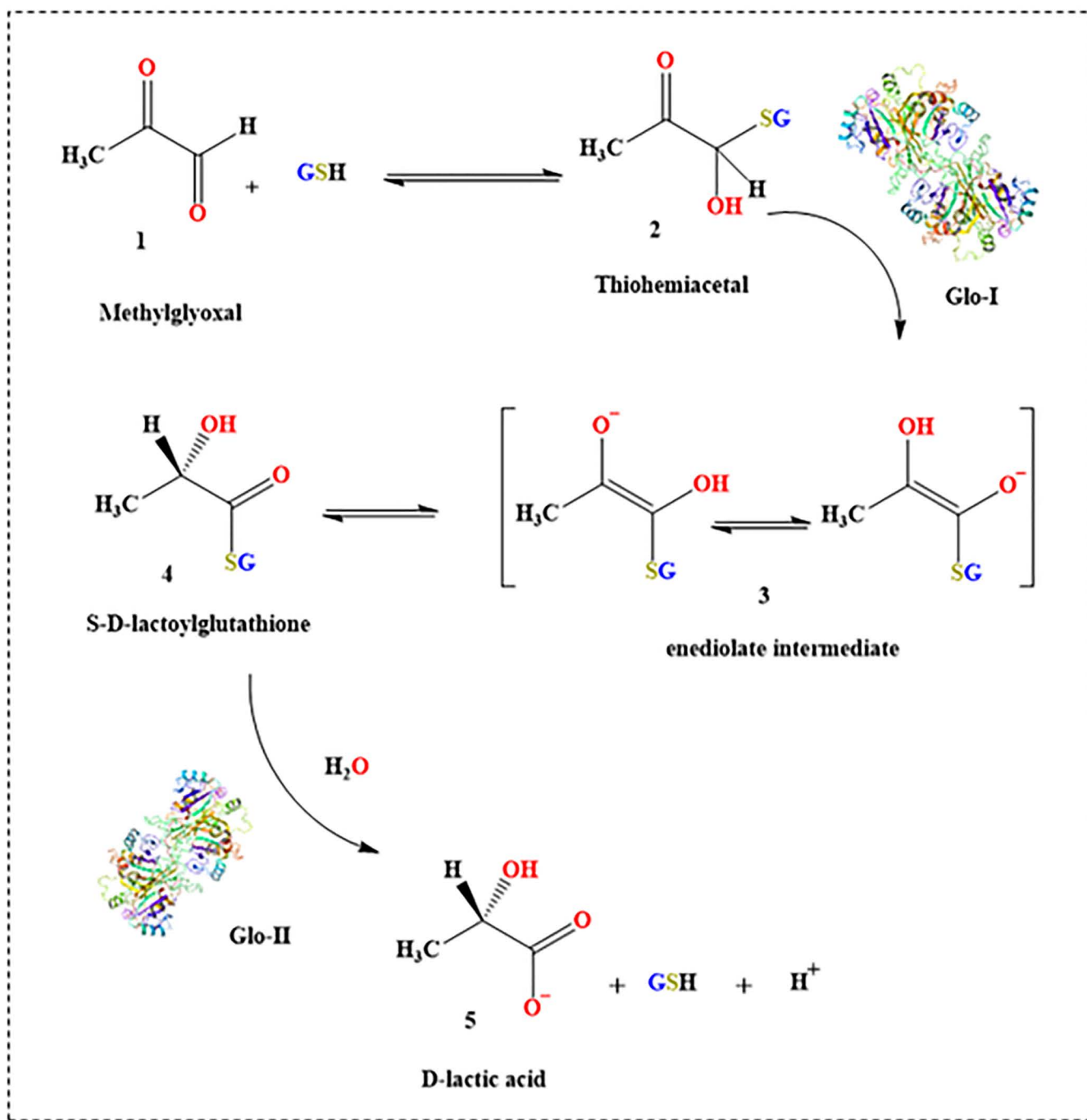


Fig 1. The role of glyoxalase system in methylglyoxal detoxification.

<https://doi.org/10.1371/journal.pone.0333405.g001>

pathways [11,17–26]. Unequivocally nutritional Intervention of glyoxylase were underscored as prominent anti-Ageing strategies and glyoxalase I mimetics were principally considered as novel anti-glycation therapeutic agents [11,12,18–29].

Inflammation triggers the onset and progression of carcinogenesis. In the inflammatory tumor microenvironment, polarized inflammatory cells have the ability to release cytokines, chemokines, and prostaglandins. This secretion serves to

stimulate tumor development, angiogenesis, and metastasis [27,30]. Undoubtedly, non-steroidal anti-inflammatory drugs (NSAIDs) significantly decreased the likelihood of developing colon adenomas, breast, prostate, and lung malignancies [31]. Cerivastatin exhibits superior dual cytotoxicity and anti-inflammatory effects compared to the other 8 lipophilic statins. This is attributed to its ability to chelate with 3,5-dihydroxyheptanoic acid [32]. Emodin was discovered to suppress inflammation, carcinogenesis, and the advancement of cancer in an animal model of colitis-associated intestinal tumorigenesis [33]. In vitro studies have shown that new fluoroquinolones with a C7-C8 ethylene diamine bridge, which are bidentate chelators have potential antioxidant, anti-inflammatory, and cytotoxic properties in a wide range of cancer cell lines [34].

Furthermore, Oxidative Stress is strongly linked to neurological illnesses, chronic inflammation, metabolic problems, and the growth, survival, and migration of malignancies [35]. ROS can primarily contribute to the occurrence of genomic instability and proapoptogenesis thereafter. Chronic inflammation can be triggered by factors such as obesity, smoking, infections, and exposure to environmental pollutants [36]; IL-1 primarily contributes to the initial phases of cancer development and the generation of reactive oxygen and nitrogen species (ROS and RNS). Additionally, it was discovered that it promotes the growth of cancerous cells and the buildup of mutations, intensifying the ability of tumor cells to spread, triggering angiogenesis, and causing the release of substances that support the growth of blood vessels and the spread of cancer. Given Oxidative Stress and Glyoxalase Pathway in Cancer development and dissemination; the involvement of antioxidants in the management and pathology of cancer is yet to be delineated [11,12,18–29,37,38]. According to findings from translational medicine, antioxidants that fight cancer can come from both natural and artificial sources. The comprehensive understanding of the molecular and cellular mechanisms underlying tumor-promoting pro-oxidative inflammation is crucial for the advancement of chemotherapy and chemoprevention strategies [39–48].

After achieving successful inhibition, additional research has been undertaken on cell lines and more sophisticated testing methods, including the assessment of anti-inflammatory and anti-oxidant properties along with assessing antiglyoxylase qualities were conducted.

Materials and methods

Selection criteria

The compounds that were examined in this study were selected based on specific criteria, including their capacity to coordinate metal ions, particularly zinc (Zn) atoms, in various enzymes within our body. SAHA (Vorinostat), trichostatin A (TSA), and acetazolamide are drugs that have been identified as potent zinc coordinators, as stated in the literature. Cimetidine works as a ligand for iron and copper, while Tolcapone binds with magnesium [49–52]. Furthermore, it has been previously reported that chemical compounds containing a catechol moiety, dihydroxy and trihydroxy benzene, exhibit inhibition of the Glo-I enzyme [53,54]. Additionally, chemicals with functional groups capable of coordinating with zinc, such as hydroxamic acid, sulfur, carboxylic acid, amide, or 3-hydroxy-4-pyridone, as well as chemicals containing a ketol moiety, were anticipated to exhibit some level of action against our intended target. The efficacy of these drugs was evaluated in vitro against Glo-I. Several drugs have been demonstrated to exhibit activity against our specific target. The active compounds underwent docking using LibDock and CDocker algorithms to determine their scores and visualize their binding interaction with the active site.

Glyoxalase-I (Glo-I) enzyme inhibition assay

Solvents and chemicals were procured from Sigma-Aldrich Co. and Acros (ThermoFisher Scientific, New Jersey, USA). The study used a human recombinant Glo-I enzyme (rhGlo-I) that was produced using *E. coli* and had an N-terminal Met and 6-His tag. The enzyme was obtained from R&D Systems® Corporation in the USA. Synthetic compounds were tested for their inhibitory effects on the enzyme using a 10mM DMSO stock concentration in triplicates. The manufacturer's protocol from R & D Systems, Inc. in Minneapolis, MN, USA was followed for the in vitro experiments. The reconstituted Glo-I enzyme (0.5mg/mL) was thawed after being stored at -70°C in sterile deionized water. The sample was observed

using a microplate reader (SpectraMax Plus by Molecular Devices, Hampton, NH 03842, USA) in a 96 well plate. The monitoring was done at a wavelength of 240 nm for 200 seconds at 37°C. The substrate mixture was freshly concocted with a concentration of 100 mM glutathione and 100 mM methylglyoxal (MG) in assay buffer containing 0.5 M sodium phosphate dibasic/monobasic. It was then left undisturbed at room temperature for 15 minutes -duration of. The selected compounds for investigation are subsequently produced in testing concentration ranges using a 0.1 M solution of sodium phosphate dibasic/monobasic with a pH range of 7–7.2. The blank contained an assay buffer with MG substrate. The test compounds were combined with human recombinant Glo-I (50 μ M) in a 96-well plate to determine their kinetic behavior. The IC_{50} values were then obtained by measuring the percentage of enzyme inhibition and comparing them to myricetin [11,18,19,21–26,54–58].

Viability assays for antiproliferative capacities of test compounds

Sulforhodamine B (SRB) assay. The cancer cell lines were cultured in DMEM supplemented with 10% FBS (Bio Whittaker, Verviers, Belgium), HEPES Buffer (10 mM), gentamicin (50 μ g/mL), L-glutamine (100 μ g/mL), streptomycin (100 mg/mL), penicillin (100 μ g/mL), and 4-(2-hydroxyethyl)-1-piperazineethanesulfonic acid (HEPES) Buffer (Sigma, St. Luis, MO, USA). The Sulforhodamine B used was obtained from Santa Cruz Biotechnology, Inc. in Texas, USA. We obtained the following cell lines for cytotoxicity screening: Human PC3 prostate cancer cell line (ATCC® CRL-1435), A375 human skin cancer cell line (ATCC® CRL-1619), A549 lung cancer cell line (ATCC® CCL-185), Breast cancer cell line MCF7 (ATCC® HTB-22), T47D (ATCC® HTB-133), HeLa uterine cervix adenocarcinoma cell line (ATCC® CRM-CCL-2), PANC1 pancreatic cell line (ATCC® CRL-1469), and colorectal cancer cell lines HT-29 (ATCC® HTB-38), HCT116 (ATCC® CCL-247), SW480 (ATCC® CCL-228), SW620 (ATCC® CCL-227), and CACO2 (ATCC® HTB-37). Periodontal ligament fibroblasts (PDL) were utilized to assess specific cytotoxicity. Cancer cell lines that have survived offer several benefits. They provide a consistent and uninterrupted source of cells, so bypassing any ethical concerns related to the use of human tissue. Additionally, they are cost-effective [59]. The cytotoxicity levels were assessed using the Sulforhodamine B (SRB) colorimetric assay, provided by Santa Cruz Biotechnology, Inc. in Texas, USA. The Spectro Scan 80D UV-VIS spectrophotometer, manufactured by Sedico Ltd. in Nicosia, Cyprus, was employed for this cytotoxicity screening [60–65]. The cells were co-incubated with substances or a reference agent at various doses ranging from 5 to 200 μ g/mL. Cisplatin, a potent and traditional anticancer drug that induces programmed cell death, was used as a reference agent at concentrations ranging from 1 to 200 μ M for the purpose of comparison. The reduction in cell viability was analyzed by plotting Dose-response curves and expressing the data as a percentage of the control optical density. The IC_{50} values were obtained using regression analysis. The anti-proliferative activities were determined as the mean IC_{50} concentrations of the investigated compounds, along with the standard deviation (SD) (n=12) [66–72].

Anti-inflammatory (nitrite) determination *in vitro*. The RAW 264.7 mouse macrophage cell line (ATCC® TIB-71) was cultivated in high glucose DMEM with 10% foetal bovine serum (FBS), 100 U/mL penicillin, 100 μ g/mL streptomycin, and 100 μ g/mL L-glutamate. The cells were incubated at 37°C in a humidified environment with 95% air and 5% CO₂. Confluent macrophages (2 x 10⁵/well) were cultured with lipopolysaccharide (LPS; 20 μ g/mL; Sigma, St. Luis, MO, USA) and indomethacin (25–200 μ g/mL) as the positive control, along with various concentrations (5–200 μ g/mL) of treatment compounds. The cells were incubated for 24 hours. 100 μ L of Griess reagent were combined with 100 μ L portions of cell culture medium and left to incubate at room temperature for 10 minutes. The absorbance at a wavelength of 550 nm was measured using a microplate reader, namely the Spectro Scan 80D UV-VIS spectrophotometer manufactured by Sedico Ltd. in Nicosia, Cyprus. The nitrite concentration was assessed by comparing it to a standard curve of sodium nitrite. A cytotoxicity protocol using SRB was conducted to assess the impact of the test substances under study on RAW 264.7 viability [70–72].

DPPH free radical scavenger assay. This approach relies on the reduction of the radicals, which causes a change in colour from oxidized purple to reduced yellow. Primarily, Diphenyl-2-picryl-hydrazone (DPPH) is reduced in a solution of methanol (MeOH)

when a chemical that donates hydrogen is present. This reduction is due to the creation of the non-radical form DPPH-H. The alteration in colour can be precisely assessed by employing a spectrophotometer within the wavelength range of 515–520 nm. Unlike other assays for radical scavenging, the DPPH radical is stable and yields consistent spectroscopic data. A 0.2 mM DPPH solution was diluted with MeOH and then combined with treatment compounds and ascorbic acid in a 1:1 concentration ratio using a 96-well plate. This resulted in a final concentration range of 6.25–200 µg/mL for the test agents. The solution was then incubated for one hour, isolated from light. Subsequently, the alteration in absorbance at a wavelength of 517 nm was quantified using a microplate reader manufactured by Bio-Tek Instrument in the United States. Ascorbic acid served as a strong and traditional benchmark for comparing the effectiveness of radical scavenging agents. The DPPH radical scavenging activity inhibition was calculated using the following equation, where A denotes photometric absorbance: The formula to calculate the percentage difference between a control and a sample is: (A control – A sample)/ A control x 100% [71,72].

Computational methods

The compounds that demonstrated efficacy against our target were analyzed using the LibDock and CDocker algorithms in Biovia® Discovery Studio 2022. Human Glo-I enzyme structural models were downloaded from the RCSB Protein Data Bank. The crystal form with the PDB ID: 3W0T was selected as the working model due to its resolution of 1.35 Å—the highest among the reported Glo-I structures—offering the most accurate and comprehensive atomic information. The downloaded protein, crystallized, was processed with the “Prepare Protein” tool in BIOVIA Discovery Studio. The tool was used for correcting and refining the structure by eliminating common crystallographic errors, Structural modifications included filling in missing parts, optimizing flexible regions, and fixing chemical properties to physiological pH. Finally, the structure was energy-minimized to eliminate steric collisions and optimize the overall geometry to verify that it was suitable for subsequent computational modeling and simulation work. The seven compound was established for prepare and generate ligand using the “Prepare Ligand” tool of BIOVIA Discovery Studio. Ligand conformations were optimized, protonation state at physiological pH corrected, 3D structure created and tautomers in the process. The elimination of duplicate or problematic entries was also performed. Ligands were minimized with the CHARMM force field and the smart minimizer to position them in a stable, low-energy form in preparation for docking studies [73]. Molecular docking studies were conducted to evaluate the binding pose and interaction energy of the prepared Glo-I protein structure with the selected ligand molecules. Docking was initially performed using the LibDock module of BIOVIA Discovery Studio based on a site-featured algorithm, which aligns ligands with protein interaction hot spots—polar and apolar regions in the binding site. Default parameters were applied, with modifications to docking performance (High Quality Protocol), conformation method (Best), and minimization (Do Not Minimize). Predicted poses were assessed based on interaction energies and significant contacts with active site residues. For further validation of binding interactions, docking was also carried out with CDocker protocol using CHARMM force field, charging ligand partial charges via the Momany-Rone method. The generated poses were visually inspected to determine how well they fit into the active site and the quality of their interactions with important residues, in support of further consideration of their potential activity.

Statistical analysis

The values were presented as mean ± SD of 12 independent experiments (per each design) and were determined using GraphPad Prism software [version 8.0 for Windows; GraphPad software, San Diego, CA, USA].

Results and discussion

Glo-I active compounds

The active compounds targeting the Glo-I enzymes were classified into two groups: highly active compounds and compounds with intermediate activity, based on their in vitro results as presented in [Table 1](#) and illustrated in [Fig 2](#). The

Table 1. The inhibitory activity of the most active compounds against Glo-I enzyme with less than 50 μ M. Their supportive corresponding docking values on two different protocols are displayed.

Name	IC_{50} μ M \pm SD	LibDock score	- CDocker interaction energy
#1 4-hydroxy-estradiol	0.226 \pm 26.43	95.88	32.87
#2 Shikonin	8.1 \pm 29.25	109.41	42.89
#3 Tolcapone	9.6 \pm 32.97	97.14	40.82
#4 Quinalizarin	33.4 \pm 12.64	101.92	31.29
#5 Hispidine	36.4 \pm 16.14	94.59	34.48
#6 Trichostatin A	43.5 \pm 15.61	109.18	25.04
#7 Calceolarioside A	44.3 \pm 18.64	147.64	58.94
Positive control (Myricetin)	3.6 \pm 36.28	123.69	56.07

<https://doi.org/10.1371/journal.pone.0333405.t001>

compounds with an IC_{50} value below 10 μ M are considered highly active, whereas those with values between 10 μ M and 50 μ M are classified as intermediate.

4-hydroxyestradiol is a naturally occurring catechol estrogen that is produced as a minor metabolite of estradiol. It has estrogenic properties that closely resemble other hydroxylated estrogen metabolites, including 2-hydroxyestradiol, 16-hydroxyestrone estriol (16-hydroxyestradiol), and 4-hydroxyestrone [74]. Furthermore, it has been identified as a highly effective inhibitor of the Glo-I enzyme, displaying an activity level of 0.22 μ M. Consequently, it holds promise as a prospective candidate for use as an anticancer agent. Fig 3 illustrates the binding pattern of this chemical. As anticipated, the catechol moiety engages in interactions with the zinc atom located in the active site, whereas the hydroxyl group at position 17 interacts with the amino acid Met 157 at the entrance of the active site. The hydrophobic structure of the steroid molecule engages in hydrophobic interactions with the non-polar amino acids at the active site, specifically Leu69 and Phe62.

Shikonin and its derivatives are obtained from traditional medicinal plant species belonging to the Boraginaceae family. They were frequently employed in ancient medical practices to address a wide range of ailments, including but not limited to cancer, blood clot prevention, protection of nerve cells, diabetes management, viral infection control, and reduction of inflammation [75]. Additionally, it demonstrates strong inhibitory effects on the Glo-I enzyme, with an activity level of 8.1 μ M, suggesting its potential as an anticancer medication. Fig 4 reveals an unexpected interaction between the terminal aliphatic OH group and the zinc atom, while the hydrophobic arm occupies the hydrophobic pocket. The keto moiety, known for its ability to coordinate with zinc, is unable to fulfil its function due to being tightly confined within the hydrophobic pocket, far from the zinc atom. The hydrophobic arm interacts with the hydrophobic amino acids located near the entrance, as anticipated. Also, it augments the potency of binding at the active site by forming hydrogen bonds with Cys 60.

Tolcapone functions as a catechol-O-methyltransferase (COMT) inhibitor, which is a crucial enzyme involved in the metabolic pathway of levodopa. It is used as a supplement to levodopa/carbidopa treatment in the control of Parkinson's disease [76]. With a potency of 9.6 μ M against the Glo-I enzyme, it demonstrates strong inhibitory activity, indicating its effectiveness as an enzyme blocker and its potential as an anticancer medicine. Fig 5 illustrates the binding pattern of this chemical. The ketone and nitro groups directly bind to the zinc atom in the active site, as demonstrated. Furthermore, the

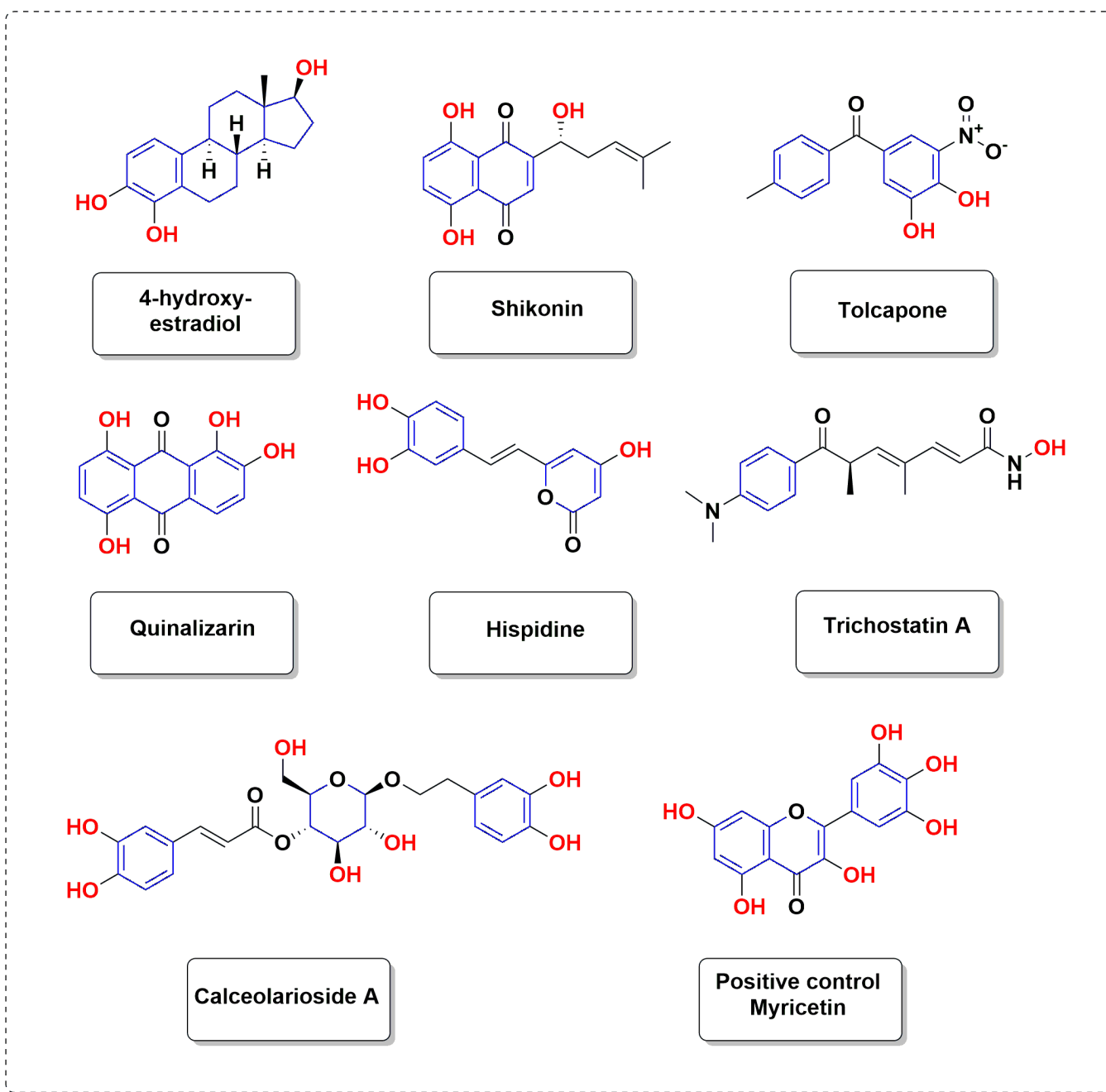


Fig 2. Active compounds identified as glyoxalase-I inhibitors.

<https://doi.org/10.1371/journal.pone.0333405.g002>

nitro group engages in hydrogen bond interactions with the amino acid Thr101 near the entrance of the active area. The benzene rings engage in hydrophobic interactions with non-polar amino acids in the active site, namely Leu 69, Phe 62, and Phe162.

Trichostatin A (TSA), a fungal antibiotic derived from *Streptomyces*, functions as a potent inhibitor of mammalian histone deacetylases, particularly the class I and II families of enzymes. TSA has been demonstrated to elicit an inhibitory

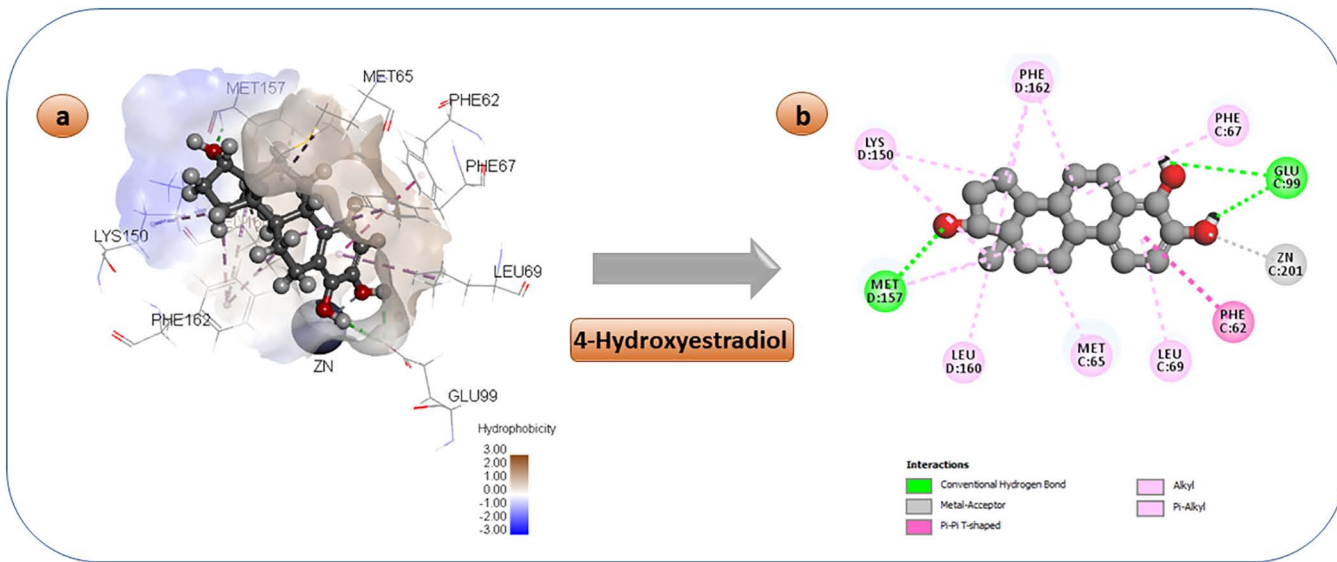


Fig 3. 3D and 2D pose of the docked 4-hydroxyestradiol diagram displaying a variety of interactions with enzyme's active region.

<https://doi.org/10.1371/journal.pone.0333405.g003>

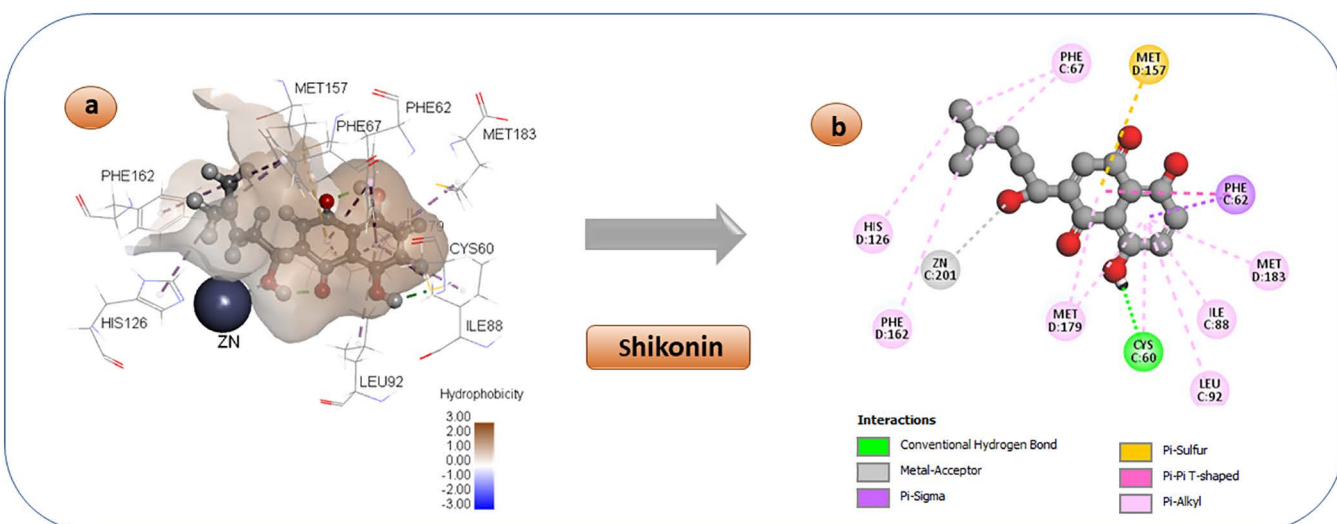


Fig 4. 3D and 2D pose of the docked Shikonin diagram displaying a variety of interactions with enzyme's active region.

<https://doi.org/10.1371/journal.pone.0333405.g004>

response in the growth of certain types of cancers [77]. The presence of a hydroxamic acid group as a zinc coordinator in the compound may account for its moderate activity (43.5 μ M) against the Glo-I enzyme. Calceolarioside A, a phenyl-propanoid glycoside previously detected in multiple Calceolaria species. It exhibits antinociceptive effects and possesses anti-inflammatory properties [78]. Furthermore, it exhibited moderate inhibition against Glo-I with an IC_{50} value of 44.3 μ M, which is believed to be attributed to the presence of a catechol moiety. Quinalizarin is a hydroxy-9, 10-anthraquinone derivative that belongs to the family of anthracycline anticancer medications. It also acts as a protein kinase inhibitor [79]. The presence of a ketol moiety in the compound is likely responsible for its modest activity (33.4 μ M) as it is expected to bind to zinc. Hispidin (HIP) is widely present in edible mushrooms, and several studies investigating its potential

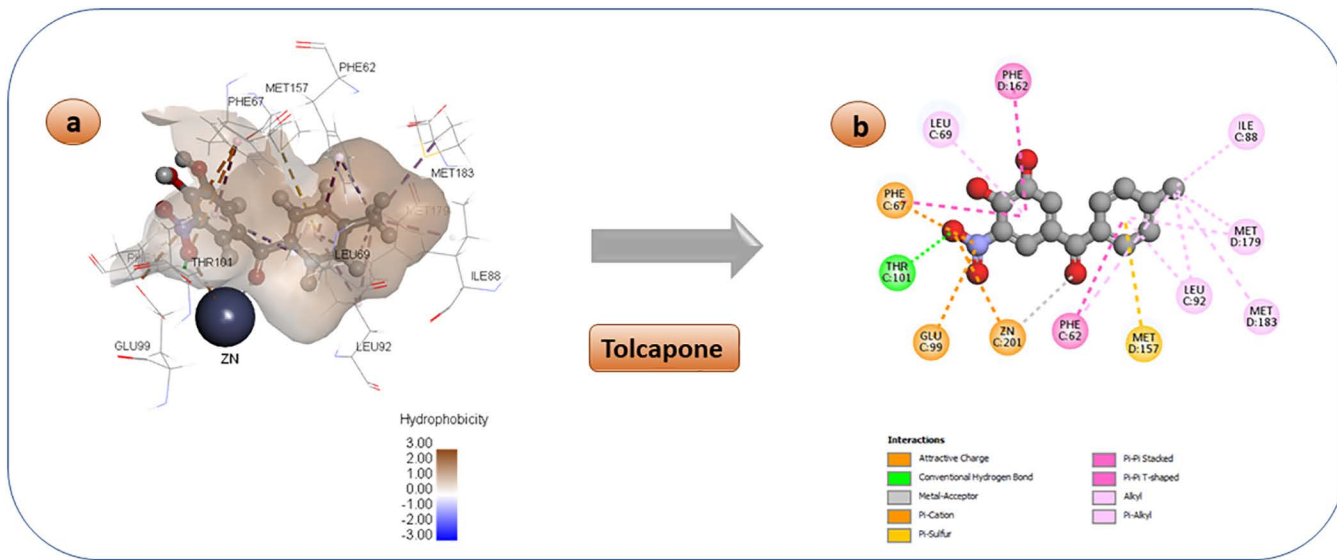


Fig 5. 3D and 2D pose of the docked Tolcapone diagram displaying a variety of interactions with enzyme's active region.

<https://doi.org/10.1371/journal.pone.0333405.g005>

pharmacological advantages have been published [80,81]. Prior studies have demonstrated that HIP exhibits antioxidant capabilities, as well as anti-inflammatory, anticancer, and antiallergic effects, among other benefits. Furthermore, it exhibited moderate activity against Glo-I, with an IC_{50} value of (36.4 μ M), which is believed to be associated with the catechol component [82–86].

Inactive compounds

The inactive compounds were categorized into various groups based on their functional groups, as seen in Fig 6. The first group in box A consists of a hydroxyl moiety that is linked to either an aromatic ring, a monocyclic conjugated ring, or a non-aromatic ring. The second group in box B consists of dihydroxy groups that are distinct from both catechol and trihydroxy groups. The third group in box C consists of catechol compounds that have either one or two carboxylic acid derivatives or amine carboxylic acid derivatives, with varying molecular weights. Box D has a methoxy group that is generated by methylating catechol groups. Furthermore, Box F has a hydroxamic acid group, which likewise serves as zinc coordinators. Box G has a nitrile functional group that serves as a zinc coordinator. Box H comprises several zinc coordination functional groups.

In details, the chemical moieties vary in size, ranging from small to large. The inactive compounds were categorized according to their size. Small-sized compounds, such as Tropolon, 3-Hydroxy-1,2-dimethyl-4(1h)-pyridone, Chloric acid, and Dimethylglyoxime, may not be able to enter the active site due to their high polarity. Even if they do manage to enter, they will not be able to fully inhibit the activity. Conversely, bigger molecules such as cynarine and 3,4-diaffeoylquinic acid are anticipated to have reduced activity since their size exceeds that of the active site. Consequently, molecules are unable to gain access to the active site and engage with it effectively.

It was anticipated that highly ionized compounds, such as Benserazide, Higenamine, and n,n-bis (alpha-cyano-4-dimethylaminobenzyl)ethylenediamine, would be ineffective because the ionizable amine group present in them is repelled by positively ionized amino acids near the entrance of the active site. Polar molecules such as caftaric acid, chrosmic acid, and withaferine A may face difficulty in reaching the active site because of the significant solvation penalty.

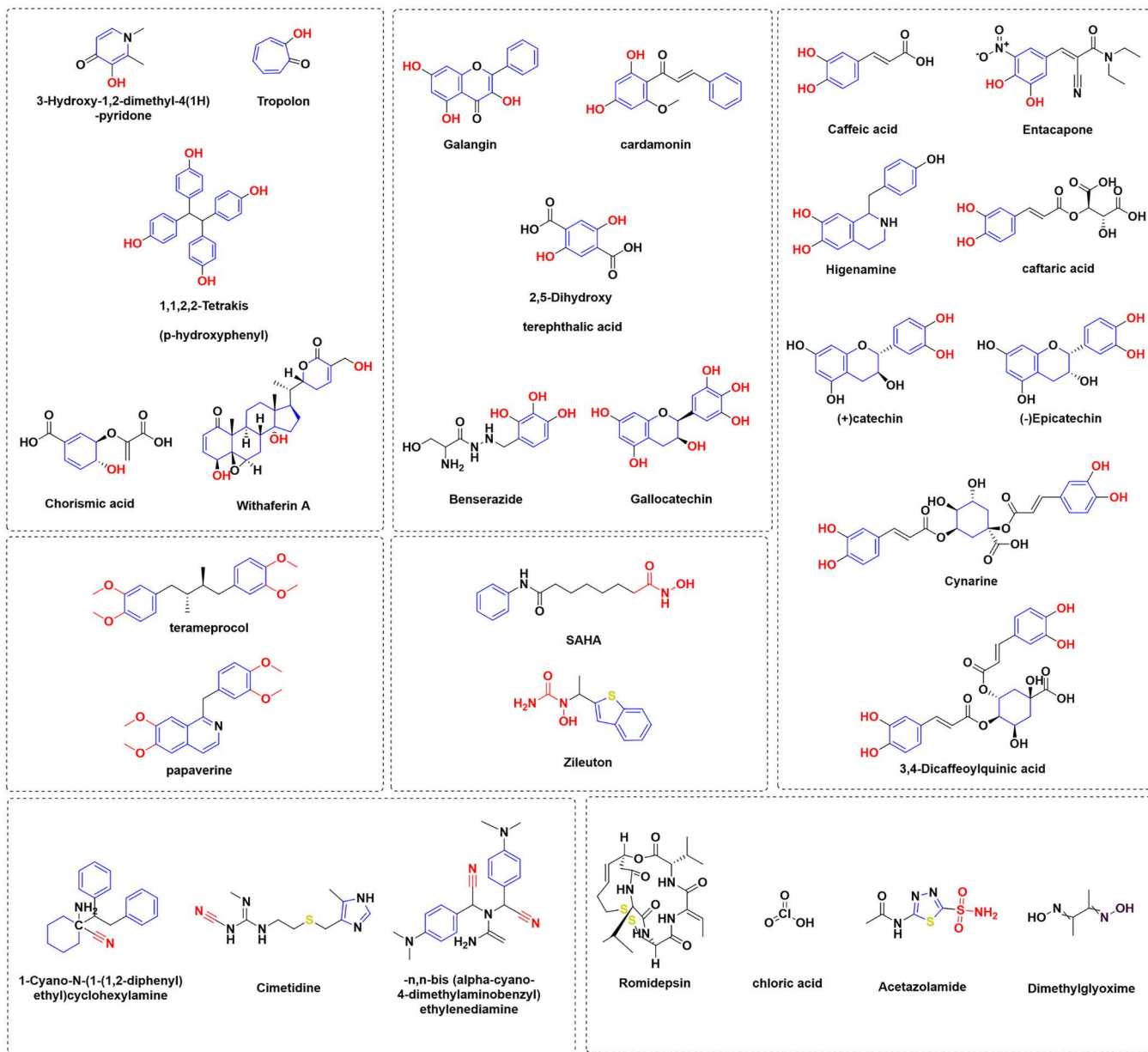


Fig 6. Classification of inactive compounds.

<https://doi.org/10.1371/journal.pone.0333405.g006>

The selection of Terameprocol was based on its resemblance to the highly potent molecule (4,4'-(2R,3S)-2,3-dimethylbutane-1,4-diyl)bis(benzene-1,2-diol)), as described in a prior publication with an IC_{50} value of 36.5nM. Terameprocol is rendered inactive due to the substitution of the catechol moiety with a methoxy group. By methylating catechol to form methoxy, the compounds were rendered inactive. This provides compelling evidence that the catechol moiety plays a crucial function in binding to the zinc atom [87].

SAHA and Zileuton exhibit potent zinc coordination via a hydroxamic acid group, but regrettably, they do not demonstrate efficacy against Glo-I. This can be ascribed to the compounds' incapacity to align with the geometric structure of

the active site. The compounds Gallocatechin, (+)Catechin, and (-)Epicatechin are inactive, possibly due to the presence of a chiral center in their molecules. This chiral center hinders appropriate binding, as previously demonstrated by our research group [21,88]. Cimetidine was selected because to its inclusion of the imidazole ring, which is recognized for its capacity to bind zinc, similar to the histidine amino acid. The imidazole ring appears to be incapable of coordinating with the zinc atom. The reduction of activity in Entacapone compared to Tolcapone (active) can be attributed to the presence of cyano and the substitution of toluene with diethyl tertiary amide. This loss of activity may be explained by the adoption of an inappropriate geometry [75].

Box H contains known chemicals capable of coordinating with zinc, such as acetazolamide, a carbonic anhydrase inhibitor (CAI). The compound contains sulphonamide functionality, which forms a bond with the zinc atom located within the active site of (CAI). However, it did not exhibit any action against Glo-I [89]. This suggests that although these medicines possess a zinc coordinating functional group, they exhibit selectivity towards their intended target and are incapable of inhibiting Glo-I action.

Glyoxalase I (Glo-I) inhibition as novel and successful molecular mechanism of cytotoxicity in vitro

Tables 2 and 3 demonstrate that doxorubicin exhibited significant inhibitory effects on cell proliferation, with IC_{50} values ranging from 0.006 μ M to less than 7.2 μ M, in cancerous monolayers of gastrointestinal (colorectal and pancreatic), skin, lung, prostate, cervical, and mammary tissues. The SRB bioassay was employed to evaluate the effects of cisplatin on the viability of cancer monolayers. Cisplatin demonstrated significant dose-dependent reductions in viability, with IC_{50} values ranging from 1.9 to 33 μ M. Remarkably similar to doxorubicin (Table 2), all relevant selective lack of cytotoxicities were evident in normal PDL fibroblasts by 72 h incubations of all phytoprinciples, further supportive of their physiologically regulated efficacies [89]. Basically, these effects were in contrast to cisplatin's lack of selective cytotoxicity. Impressively Table 2 shows that trichostatin A, along with other phytoprinciples, significantly inhibited the development of colorectal and pancreatic cancer cells. Trichostatin A demonstrated a strong inhibitory impact with IC_{50} values of $\leq 27 \mu$ M after 72 hours of incubation. Phytomedicine-derived bioactive compounds have demonstrated highly effective viability reduction capabilities (with IC_{50} values $\leq 100 \mu$ M) in colorectal cancer cell lines CACO2, SW480, HCT116, SW620, and HT29. However,

Table 2. Cytotoxicity (as of %Control) IC_{50} value (mean \pm SD in μ M) of the tested compounds vs. Positive controls Cisplatin and doxorubicin against gastrointestinal and colorectal malignancies' adherent monolayers.

Treatment	CACO2	SW480	HCT116	SW620	HT29	PANC1	PDL fibroblasts
4-Hydroxyestradiol	106.58 \pm 4.77	109.45 \pm 6.86	124.3 \pm 7.8	142.29 \pm 16.5	118.35 \pm 4.17	66.9 \pm 2.69	NI***
Trichostatin	27.05 \pm 1.28	44.34 \pm 4.67	14 \pm 2.5	19.5 \pm	27 \pm 0.85	95.8 \pm 8.2	NI***
Calceolarioside A	NT**	NT**	NT**	NT**	NT**	NT**	NI***
Quinalizarin	108.55 \pm 9.26	117.75 \pm 3.04	72.2 \pm 5.7	40.68 \pm 2.21	143.85 \pm 15.6	127.42 \pm 2.52	NI***
Shikonin	43.82 \pm 4.97	41.63 \pm 6.37	108.2 \pm 2.6	60.27 \pm 2.07	142.26 \pm 0.76	80.01 \pm 2.11	NI***
Telcapone	94.8 \pm 6.65	164.95 \pm 6.58	86.2 \pm 6.6	105.4 \pm 8.35	63.28 \pm 1.03	119.07 \pm 9.28	NI***
Hispidin	74.3 \pm 1.13	34.6 \pm 3.11	198.5 \pm 12.2	34.26 \pm 6.52	82.75 \pm 0.78	129.8 \pm 2.08	NI***
MYRICETIN	106.5 \pm 0.6	88.93 \pm 14.11	44.71 \pm 2.14	42.75 \pm 0.78	32.65 \pm 1.06	197.64 \pm 43	NI***
Cisplatin	4.88 \pm 0.59	2.6 \pm 0.14	1.92 \pm 0.14	10 \pm 0.6	3.35 \pm 0.21	11.82 \pm 0.25	5.6 \pm 0.53
Doxorubicin	0.92 \pm 0.03	0.01 \pm 0.00	0.92 \pm 0.03	0.65 \pm 0.03	0.006 \pm 0.000	7.17 \pm 1.07	NI***

Notes: Results are mean \pm SD (n=12). IC_{50} values (concentration at which 50% inhibition of cell proliferation took place in comparison to non-induced basal 72 h incubations) were calculated within 0.1–200 μ M range. Lack of cytotoxicity of the same panel of tested compounds against normal PDL (periodontal ligament) fibroblasts vs. cisplatin and doxorubicin.

NT:**Not tested.

NI*** Non-inhibitory within testing dose range”.

<https://doi.org/10.1371/journal.pone.0333405.t002>

Table 3. Cytotoxicity (as of %Control) IC_{50} value (mean \pm SD in μ M) of the tested compounds vs. positive controls Cisplatin and doxorubicin against other malignancy' cell lines adherent monolayers.

Treatment	A375 skin melanoma	A549 lung malignancy	PC3 prostate malignancy	MCF7 mammary malignancy	T47D mammary malignancy	HeLa cervix malignancy
4-Hydroxyestradiol	47.1 \pm 1.9	15.15 \pm 1.34	82.25 \pm 8.56	139.8 \pm 1.13	51.53 \pm 5.2	29.75 \pm 4.74
Trichostatin	5.6 \pm 0.6	2.0 \pm 0.21	47.5 \pm 3.96	2.25 \pm 0.49	14.7 \pm 0.28	1.4 \pm 0.2
Calceolarioside A	NT**	NT**	NT**	899.25 \pm 179.25	45.65 \pm 3.46	207.6 \pm 34.78
Quinalizarin	48.6 \pm 1.8	7.9 \pm 0.71	143.08 \pm 0.18	33.25 \pm 0.78	37.72 \pm 4.78	85.51 \pm 0.44
Shikonin	56.5 \pm 6.9	54 \pm 5.8	176.22 \pm 1.25	37.75 \pm 3.89	30.91 \pm 3.66	13.87 \pm 1.91
Tolcapone	64.1 \pm 1.1	61.96 \pm 2.21	256.68 \pm 37.11	25.56 \pm 1.49	26.85 \pm 0.35	39.35 \pm 0.35
Hispidin	98.9 \pm 9	26.02 \pm 5.22	138.81 \pm 13.58	384.15 \pm 7.57	52.63 \pm 0.69	122.45 \pm 1.34
MYRICETIN	51.7 \pm 4.1	27.46 \pm 4.47	65.4 \pm 1.84	73.05 \pm 0.78	29.8 \pm 2.6	35.8 \pm 4.4
Cisplatin	15.7 \pm 0.6	33.03 \pm 2.49	6.27 \pm 0.95	12.8 \pm 1.98	12.15 \pm 0.35	22.75 \pm 1.2
Doxorubicin	0.28 \pm 0.14	0.28 \pm 0.00	0.13 \pm 0.01	4.81 \pm 0.21	0.02 \pm 0.00	5.56 \pm 0.08

Notes: Results are mean \pm SD (n = 12). IC_{50} values (concentration at which 50% inhibition of cell proliferation took place in comparison to non-induced basal 72h incubations) were calculated within 0.1–200 μ M range. NT: **Not tested.

<https://doi.org/10.1371/journal.pone.0333405.t003>

the investigated plant chemicals showed significantly lower levels of cytotoxicity in PANC1 pancreatic cancer adherent monolayers.

[Table 3](#) demonstrates that Trichostatin exhibited significantly higher cytotoxicity affinities, with IC_{50} values below 10 μ M, compared to cisplatin, and similar to doxorubicin, in skin melanoma, lung carcinoma, mammary, and cervix adenocarcinomas. The remaining phytoprinciples exhibited significantly moderate antiproliferative effects (with IC_{50} values <50 μ M) in cancer cell lines including cutaneous A375, mammary T47D and MCF7, and cervical HeLa. The prostate PC3 72h incubations showed the lowest effectiveness in reducing viability when using repurposed phytoprinciples. However, the most significant effectiveness, with IC_{50} values less than 25 μ M compared to cisplatin's 33 μ M, was observed in adenocarcinoma monolayers.

Glyoxalase I (Glo-I) inhibitors as novel and successful dual antiinflammation-cytotoxicity natural agents

[Table 4](#) presents the significantly moderate abilities of phytoprinciples to scavenge DPPH radicals and act as antioxidants, compared to the capabilities of ascorbic acid (with IC_{50} values ranging from 25 μ M to 100 μ M). Furthermore, all naturally occurring substances exhibited significant anti-inflammatory effects that were comparable to those of the nonsteroidal anti-inflammatory drug indomethacin, as shown in the same table. All IC_{50} values were maintained at levels below 10 μ M, which is a notable achievement. Myricetin had a remarkably strong ability to reduce inflammation, with an IC_{50} value of 50 nM. None of the evaluated medications' efficacies were significantly correlated with reductions in viability as validated by SRB [90–97].

It is important to note that, except for Trichostatin A, the most effective compounds against Glo-I, such as 4-hydroxy-Estradiol, Shikonin, and Tolcapone, have similar structural characteristics. They all possess at least one free Zn chelating group, which includes catechol groups or betahydroxy ketone. The exceptional inhibitory effect of Myricetin against Glo-I can be attributed to the presence of two Zn chelator groups. The instructions are sufficiently clear for most participants to follow by avoiding any disturbance with the proximity of Zn chelation. This was further confirmed and shown by the presence of trans-isomerism, which enforces a semi-planar/linear structure and, as a result, enhances activity. The mild cytotoxic activity of Glo-I active hits can be largely attributed to lipophilicity. There is ample evidence to support the fact that lipophilic substances readily permeate the cell membrane of cancer cells. The hydrophilic nature of our hits' structure accounts for their moderate to low cytotoxic activity.

Table 4. IC_{50} values (mean \pm SD in μ M) of *in vitro* DPPH-radical scavenging properties vs. ascorbic acid and antiinflammation propensities vs. indomethacin of the tested compounds.

Treatment	DPPH- IC_{50} value μ M	iNOS- IC_{50} value μ M
4-Hydroxyestradiol	506.35 \pm 102	0.25 \pm 0.04
Trichostatin	99.33 \pm 15.45	1.69 \pm 0.12
Calceolarioside A	NT**	NT**
Quinalizarin	579.95 \pm 26.52	1.85 \pm 0.34
Shikonin	34.37 \pm 5.04	0.27 \pm 0.05
Telcapone	92.1 \pm 2.4	1.19 \pm 0.17
Hispidin	26.26 \pm 0.65	3.47 \pm 0.49
MYRICETIN	70.73 \pm 11.64	0.07 \pm 0.01
Reference Drug	Ascorbic Acid 0.09 \pm 0.01 μ M	Indomethacin 0.02 \pm 0.00 μ M

Notes: Results are mean \pm SD (n=12). IC_{50} values (μ M) (concentration at which 50% inhibition of DPPH reduction in comparison to non-induced basal incubations) were calculated within testing dose range. Lack of cytotoxicity of the same panel of tested compounds against LPS-primed inflammation in RAW macrophages vs. indomethacin. NT: not tested.

<https://doi.org/10.1371/journal.pone.0333405.t004>

[Table 2](#) demonstrates that the majority of active hits were mostly directed towards colorectal cell lines. This can be attributed to the overexpression of Glo-I in colorectal cancer (CRC), as supported by literature [98]. Therefore, this strongly confirm Glo-I as the primary target in CRC for cancer treatment. However, [Table 3](#) displays that the majority of active hits display significantly modest abilities to inhibit the growth of cancer cells in skin A375, mammary T47D and MCF7, and cervical Hela. These findings indicate the involvement of Glo-I in these cells, along with other possible targets. Interestingly, the remarkable cytotoxicity of Trichostatin A against nearly all examined cell lines clearly indicates the significant significance of the Hydroxamic acid group, revealing additional targets such as Histone deacetylase (HDAC) receptors. The exceptional capacity of Trichostatin A to inhibit many enzymes, including Glo-I-HDAC, can account for its significant antiproliferative activity. This effect is likely due to its linear and lipophilic properties. Ultimately, this study reveals naturally occurring substances that inhibit Glo-I and have the potential to act against cancer cells.

Speculative molecular action mechanisms of antitumor -antiinflammation cross talks biology. To Speculatively elucidate the intricate linkage of inflammation- tumerogenesis relationship; naturally occurring methyl analogs of mushrooms' antcins had substantial cytotoxicities attributed to their ability to modulate signaling cascades in apoptotic pathways combined with antiinflammation capacities [99]. Reportedly Cathepsins are cysteine proteases that can be involved in regulable fundamental mechanisms as apoptosis, pyroptosis, ferroptosis, necroptosis, and autophagic cell death [100]. As they are cardiometabolic adiposity biomarker expressed in white adipose tissue; mostly elevated circulating concentrations of cathepsins can be strongly and independently associated with metabolic syndrome in overweight and obese adults [101]. Also, they are substantially involved in osteolysis, immunomodulation and apoptosis with a significant role in metastatic pancreatic cancer. In particular, targeting cathepsin subtypes was found promising in reducing tumor progression migration and invasion, further enhancing the efficacy of chemotherapeutic agents in preclinical models [102]. Recently antiproliferative α -fluorocinnamate-based cysteine protease inhibitors were principally proven as highly effective candidates targeting cathepsins in markedly reducing pancreatic cancer cell proliferation [102,103]. Interestingly chemerin, Defensin 1, and TNF α were underscored as potential biomarkers in the early diagnosis of colorectal cancer [104], tubulins can also serve the same purpose as their inhibitors being classified as anticancer agents [105]. Survivin can be an antiapoptotic peptide inhibiting caspases -3 and -7 via activation of intrinsic apoptogenic pathway [106] closely linked to antitumor immunity (Jazayeri et al., 2020) thereby underscoring rapid noninvasive detection of bladder cancer [107]. Moreover, In-depth, molecular action mechanism of cisplatin cardiotoxicity can afford translational evidence into cardioprotective effectiveness of safe antiproliferation compounds [108]. Substantial changes

to levels of proinflammatory IL-1 β , -6 and antiinflammatory IL10 and SIRT1 can be recognized in their cross-talk of mechanistic immunomodulation [109,110].

Concluding remarks and future directives. To summarize, a range of compounds were tested for their impact on Glo-I enzyme activity. The compounds that exhibited inhibitory action were then assessed for their effects on cytotoxicity, anti-inflammatory properties, and antioxidant capabilities. As a result of these assessments, 4-hydroxyestradiol was identified as a potent inhibitor against Glo-I, with an IC₅₀ value of 0.226 μ M. Unequivocally unlike undifferential cytotoxicity of cisplatin, the spectrum of safety of all tested agents in periodontal ligament fibroblasts PDL-based 72h incubations and RAW 264.7 macrophages were reportedly signified. Trichostatin exhibited notable inhibitory effects on the growth of cancer cells, leading to considerable reductions in cell viability in multiple cancer cell cultures. Nevertheless, tumour samples obtained from the prostate and pancreas exhibited remarkable resistance. Docking investigations are conducted to demonstrate the binding interactions that occur at the active site. The pharmacological properties of phytochemicals were examined in comparison to indomethacin and vitamin C, demonstrating notably remarkable anti-inflammatory effects and considerably appreciable antioxidant abilities. These findings emphasize the therapeutic potential of the compounds, including their ability to inhibit Glo-I, their anti-cancer activity, anti-inflammatory effects, and antioxidant capabilities. These insights are valuable for guiding future research in targeted therapeutic interventions.

- ⌚ As marked selective antiproliferation affinities of tested agents in cell-based assays were highly signified. Future work should be directed on synthesizing new derivatives with focus on structural betterments and augmentations further elucidating the structure-activity relationship of their remarkable pharmacologies.
- ⌚ Possible high throughput screenings of these promising naturals and new derivatives on other malignancy cell lines is certainly advised.
- ⌚ Suggestively investigating possible molecular action mechanisms of potent natural agents (proapoptogenesis, angiogenesis, anti-platelet activity vs. the appropriately selected and respective reference agents) is warranted.
- ⌚ Downstream In vivo evaluation of our derivatives for efficacy and safety cannot be overemphasized enough.
- ⌚ Likely Combinations with antineoplastic agents can further underscore chemosensitisation propensities of potent agents

Supporting information

S1 File. Supporting data of enzyme inhibition assays, including Tables 1–16 for compounds (4-hydroxyestradiol,

Shikonin, Tolcapone, Quinalizarin, Hispidin, Trichostatin A, Calceolarioside A, and Myricetin).

(DOCX)

Author contributions

Conceptualization: MohammedBashar Al-Qazzan, Qosay Al-Balas, Belal Alnajjar.

Data curation: MohammedBashar Al-Qazzan, Violet Kasabri, Belal Alnajjar.

Formal analysis: MohammedBashar Al-Qazzan, Qosay Al-Balas, Violet Kasabri.

Investigation: MohammedBashar Al-Qazzan, Qosay Al-Balas, Yusuf Al-Hiari.

Methodology: MohammedBashar Al-Qazzan, Rema AlKhateeb, Mohammed Al-Akeedi.

Project administration: MohammedBashar Al-Qazzan, Rema AlKhateeb.

Resources: Qosay Al-Balas, Violet Kasabri, Aref Zayed, Belal Alnajjar.

Supervision: Qosay Al-Balas, Violet Kasabri, Belal Alnajjar.

Validation: Yusuf Al-Hiari, Aref Zayed, Belal Alnajjar.

Visualization: MohammedBashar Al-Qazzan.

Writing – original draft: MohammedBashar Al-Qazzan, Mohammed Al-Akeedi.

Writing – review & editing: Qosay Al-Balas, Violet Kasabri, Yusuf Al-Hiari, Belal Alnajjar.

References

1. Prendergast GC, Jaffee EM. Cancer immunologists and cancer biologists: why we didn't talk then but need to now. *Cancer Res.* 2007;67(8):3500–4. <https://doi.org/10.1158/0008-5472.CAN-06-4626> PMID: 17413003
2. Siegel RL, Miller KD, Wagle NS, Jemal A. Cancer statistics, 2023. *CA Cancer J Clin.* 2023;73(1):17–48. <https://doi.org/10.3322/caac.21763>
3. Vince R, Wadd WB. Glyoxalase inhibitors as potential anticancer agents. *Biochem Biophys Res Commun.* 1969;35(5):593–8. [https://doi.org/10.1016/0006-291X\(69\)90445-8](https://doi.org/10.1016/0006-291X(69)90445-8) PMID: 5794079
4. Vince R, Daluge S. Glyoxalase inhibitors. A possible approach to anticancer agents. *J Med Chem.* 1971;14(1):35–7. <https://doi.org/10.1021/jm00283a009> PMID: 5099673
5. Geng X, Ma J, Zhang F, Xu C. Glyoxalase I in tumor cell proliferation and survival and as a potential target for anticancer therapy. *Oncol Res Treat.* 2014;37(10):570–4. <https://doi.org/10.1159/000367800> PMID: 25342507
6. Racker E. The mechanism of action of glyoxalase. *J Biol Chem.* 1951;190(2):685–96. [https://doi.org/10.1016/s0021-9258\(18\)56017-8](https://doi.org/10.1016/s0021-9258(18)56017-8) PMID: 14841219
7. Larsson A. Functions of glutathione: biochemical, physiological, toxicological, and clinical aspects. *Proceedings of the Fifth Karolinska Institute Nobel Conference;* 1982 May 23–27; Skokloster, Sweden. Raven Press; 1983. [https://doi.org/10.1016/0003-2697\(84\)90415-9](https://doi.org/10.1016/0003-2697(84)90415-9)
8. Carrington SJ. The glyoxalase enigma. The biological consequences of a ubiquitous enzyme. *IRCS Med Sci.* 1986;14:763–8. [https://doi.org/10.1016/0272-0590\(91\)90162-W](https://doi.org/10.1016/0272-0590(91)90162-W)
9. Richard JP. Kinetic parameters for the elimination reaction catalyzed by triosephosphate isomerase and an estimation of the reaction's physiological significance. *Biochemistry.* 1991;30(18):4581–5. <https://doi.org/10.1021/bi00232a031> PMID: 2021650
10. Thornalley PJ. Glutathione-dependent detoxification of alpha-oxoaldehydes by the glyoxalase system: involvement in disease mechanisms and antiproliferative activity of glyoxalase I inhibitors. *Chem Biol Interact.* 1998;111–112:137–51. [https://doi.org/10.1016/s0009-2797\(97\)00157-9](https://doi.org/10.1016/s0009-2797(97)00157-9) PMID: 9679550
11. He Y, Zhou C, Huang M, Tang C, Liu X, Yue Y, et al. Glyoxalase system: a systematic review of its biological activity, related-diseases, screening methods and small molecule regulators. *Biomed Pharmacother.* 2020;131:110663. <https://doi.org/10.1016/j.biopha.2020.110663> PMID: 32858501
12. Michel M, Hollenbach M, Pohl S, Ripoll C, Zipprich A. Inhibition of glyoxalase-I leads to reduced proliferation, migration and colony formation, and enhanced susceptibility to sorafenib in hepatocellular carcinoma. *Front Oncol.* 2019;9:785. <https://doi.org/10.3389/fonc.2019.00785> PMID: 31482070
13. Yumnam S, Subedi L, Kim SY. Glyoxalase system in the progression of skin aging and skin malignancies. *Int J Mol Sci.* 2020;22(1):310. <https://doi.org/10.3390/ijms22010310> PMID: 33396745
14. Kim J-Y, Jung J-H, Lee S-J, Han S-S, Hong S-H. Glyoxalase 1 as a therapeutic target in cancer and cancer stem cells. *Mol Cells.* 2022;45(12):869–76. <https://doi.org/10.14348/molcells.2022.0109> PMID: 36172978
15. Alhujaily M, Abbas H, Xue M, de la Fuente A, Rabbani N, Thornalley PJ. Studies of glyoxalase 1-linked multidrug resistance reveal glycolysis-derived reactive metabolite, methylglyoxal, is a common contributor in cancer chemotherapy targeting the spliceosome. *Front Oncol.* 2021;11:748698. <https://doi.org/10.3389/fonc.2021.748698> PMID: 34790575
16. Yanagi K, Komatsu T, Fujikawa Y, Kojima H, Okabe T, Nagano T, et al. Development of pathway-oriented screening to identify compounds to control 2-methylglyoxal metabolism in tumor cells. *Commun Chem.* 2023;6(1):68. <https://doi.org/10.1038/s42004-023-00864-y> PMID: 37055561
17. Syed Annuar SN, Kamaludin NF, Awang N, Chan KM. Cellular basis of organotin(IV) derivatives as anticancer metallodrugs: a review. *Front Chem.* 2021;9:657599. <https://doi.org/10.3389/fchem.2021.657599> PMID: 34368075
18. Al-Balas QA, Hassan MA, Al-Shar'i NA, Mhaidat NM, Almaaytah AM, Al-Mahasneh FM, et al. Novel glyoxalase-I inhibitors possessing a “zinc-binding feature” as potential anticancer agents. *Drug Des Devel Ther.* 2016;10:2623–9. <https://doi.org/10.2147/DDDT.S110997> PMID: 27574401
19. Aragonès G, Rowan S, Francisco SG, Whitcomb EA, Yang W, Perini-Villanueva G, et al. The glyoxalase system in age-related diseases: nutritional intervention as anti-ageing strategy. *Cells.* 2021;10(8):1852. <https://doi.org/10.3390/cells10081852> PMID: 34440621
20. Jin T, Zhao L, Wang H-P, Huang M-L, Yue Y, Lu C, et al. Recent advances in the discovery and development of glyoxalase I inhibitors. *Bioorg Med Chem.* 2020;28(4):115243. <https://doi.org/10.1016/j.bmc.2019.115243> PMID: 31879183

21. Al-Shar'i NA, Al-Balas QA, Al-Waqfi RA, Hassan MA, Alkhalifa AE, Ayoub NM. Discovery of a nanomolar inhibitor of the human glyoxalase-I enzyme using structure-based poly-pharmacophore modelling and molecular docking. *J Comput Aided Mol Des.* 2019;33(9):799–815. <https://doi.org/10.1007/s10822-019-00226-8> PMID: 31630312
22. Al-Balas QA, Al-Shar'i NA, Hassan MA. Design, synthesis and biological evaluation of potential novel zinc binders targeting human glyoxalase-I; a validated target for cancer treatment. *Jordan J Pharm Sci.* 2018;11(1):25–37.
23. Al-Oudat BA, Al-Shar'i NA, Al-Balas QA, Audat SA, Alqudah MAY, Hamzah AH, et al. Lead optimization and biological evaluation of diazenylbenzenesulfonamides inhibitors against glyoxalase-I enzyme as potential anticancer agents. *Bioorg Chem.* 2022;120:105657. <https://doi.org/10.1016/j.bioorg.2022.105657> PMID: 35152183
24. Battah S, Ahmed N, Thornalley PJ. Novel anti-glycation therapeutic agents: glyoxalase I mimetics. *Int Congr Ser.* 2002;1245:107–11. [https://doi.org/10.1016/s0531-5131\(02\)00884-1](https://doi.org/10.1016/s0531-5131(02)00884-1)
25. Al-Oudat BA, Abu Al fool BS, Audat SA, Al-Shar'i NA, Al-Balas QA, Zayed A, et al. Structural optimization and biological evaluation of quinoline/naphthalene-based glyoxalase-I inhibitors as anti-cancer candidates. *Med Chem Res.* 2024;33(10):1897–913. <https://doi.org/10.1007/s00044-024-03289-x>
26. Fetian MH, Al-Balas QA. Unraveling potential glyoxalase-I inhibitors utilizing structure-based drug design techniques. *Adv Appl Bioinform Chem.* 2024;17:21–32. <https://doi.org/10.2147/AABC.S441074> PMID: 38343400
27. Greten FR, Grivennikov SI. Inflammation and cancer: triggers, mechanisms, and consequences. *Immunity.* 2019;51(1):27–41. <https://doi.org/10.1016/j.immuni.2019.06.025> PMID: 31315034
28. Tiku NAB. Oxidative stress and glyoxalase pathway in cancer. In: Chakraborti S, Ray BK, Roychoudhury S, editors. *Handbook of oxidative stress in cancer: mechanistic aspects.* Singapore: Springer; 2022. https://doi.org/10.1007/978-981-15-9411-3_12
29. Vincenzi B, Simonetti S, Iuliani M, Cavaliere S, Napolitano A, Santini D, et al. 101P Pharmacological inhibition of glyoxalase-1 as novel therapeutic strategy to enhance trabectedin anti-tumor effect in soft tissue sarcoma preclinical models. *ESMO Open.* 2023;8(1):101138. <https://doi.org/10.1016/j.esmoop.2023.101138>
30. Xiong S, Dong L, Cheng L. Neutrophils in cancer carcinogenesis and metastasis. *J Hematol Oncol.* 2021;14(1):173. <https://doi.org/10.1186/s13045-021-01187-y> PMID: 34674757
31. Wang D, Dubois RN. The role of COX-2 in intestinal inflammation and colorectal cancer. *Oncogene.* 2010;29(6):781–8. <https://doi.org/10.1038/onc.2009.421> PMID: 19946329
32. Haj Hussein B, Kasabri V, Al-Hiari Y, Arabiyat S, Ikhmais B, Alalawi S, et al. Selected statins as dual antiproliferative-antiinflammatory compounds. *Asian Pac J Cancer Prev.* 2022;23(12):4047–62. <https://doi.org/10.31557/APJCP.2022.23.12.4047> PMID: 36579985
33. Zhang Y, Pu W, Bousquenaud M, Cattin S, Zaric J, Sun L-K, et al. Emodin inhibits inflammation, carcinogenesis, and cancer progression in the AOM/DSS model of colitis-associated intestinal tumorigenesis. *Front Oncol.* 2021;10:564674. <https://doi.org/10.3389/fonc.2020.564674> PMID: 33489875
34. Alzghoul M, AlHiari Y, Kasabri V. Unique bidentate chelators of functionalized heterocyclic fluoroquinolones with dual anti-inflammation and selective cytotoxicity via C7-C8 ethylene diamine bridge. *Curr Med Chem.* 2025.
35. Saha SK, Lee SB, Won J, Choi HY, Kim K, Yang G-M, et al. Correlation between oxidative stress, nutrition, and cancer initiation. *Int J Mol Sci.* 2017;18(7):1544. <https://doi.org/10.3390/ijms18071544> PMID: 28714931
36. Furman D, Campisi J, Verdin E, Carrera-Bastos P, Targ S, Franceschi C, et al. Chronic inflammation in the etiology of disease across the life span. *Nat Med.* 2019;25(12):1822–32. <https://doi.org/10.1038/s41591-019-0675-0> PMID: 31806905
37. Klaunig JE. Oxidative stress and cancer. *Curr Pharm Des.* 2018;24(40):4771–8. <https://doi.org/10.2174/1381612825666190215121712> PMID: 30767733
38. Zahra KF, Lefter R, Ali A, Abdellah E-C, Trus C, Ciobica A, et al. The involvement of the oxidative stress status in cancer pathology: a double view on the role of the antioxidants. *Oxid Med Cell Longev.* 2021;2021:9965916. <https://doi.org/10.1155/2021/9965916> PMID: 34394838
39. Bhosale PB, Ha SE, Vetrivel P, Kim HH, Kim SM, Kim GS. Functions of polyphenols and its anticancer properties in biomedical research: a narrative review. *Transl Cancer Res.* 2020;9(12):7619–31. <https://doi.org/10.21037/tcr-20-2359> PMID: 35117361
40. Tabrizi L, Nguyen TLA, Tran HDT, Pham MQ, Dao DQ. Antioxidant and anticancer properties of functionalized ferrocene with hydroxycinnamate derivatives—an integrated experimental and theoretical study. *J Chem Inf Model.* 2020;60(12):6185–203. <https://doi.org/10.1021/acs.jcim.0c00730> PMID: 33233887
41. Van Loenhout J, Peeters M, Bogaerts A, Smits E, Deben C. Oxidative stress-inducing anticancer therapies: taking a closer look at their immuno-modulating effects. *Antioxidants (Basel).* 2020;9(12):1188. <https://doi.org/10.3390/antiox9121188> PMID: 33260826
42. Arfin S, Jha NK, Jha SK, Kesari KK, Ruokolainen J, Roychoudhury S, et al. Oxidative stress in cancer cell metabolism. *Antioxidants (Basel).* 2021;10(5):642. <https://doi.org/10.3390/antiox10050642> PMID: 33922139
43. Ginting B. Evaluation of antioxidant and anticancer activity of *Myristica fragrans* Houtt. bark. *Pharmacogn J.* 2021;13(3). <https://doi.org/10.5530/pj.2021.13.99>
44. Li X, Wang X, Liu G, et al. Antioxidant stress and anticancer activity of peptide-chelated selenium in vitro. *Int J Mol Med.* 2021;48(2):1–15. <https://doi.org/10.3892/ijmm.2021.4986>

45. Noman OM, Nasr FA, Alqahtani AS, Al-zharani M, Cordero MAW, Alotaibi AA, et al. Comparative study of antioxidant and anticancer activities and HPTLC quantification of rutin in white radish (*Raphanus sativus* L.) leaves and root extracts grown in Saudi Arabia. Open Chem. 2021;19(1):408–16. <https://doi.org/10.1515/chem-2021-0042>
46. Amer MN, Atwa NA, Eldiwany AI, Elgammal EW, Dawoud IE, Rashad FM. Anticancer and antioxidant activities of l-asparaginase produced by local *Weissella paramesenteroides* MN2C2 strain. Egypt J Chem. 2022;65(7):409–19. <https://doi.org/10.21608/ejchem.2021.102465.4832>
47. Chaudhary V, Katyal P, Panwar H, Kaur J, Aluko RE, Puniya AK, et al. Antioxidative, anti-inflammatory, and anticancer properties of the red biopigment extract from *Monascus purpureus* (MTCC 369). J Food Biochem. 2022;46(9):e14249. <https://doi.org/10.1111/jfbc.14249> PMID: 35615960
48. Jawad KH, Hasson B. Developing strategy for a successful antioxidant, anticancer activity via an improved method prepared to porous silicon nanoparticles. J Appl Sci Nanotechnol. 2021;1(4):1–11. <https://doi.org/10.53293/jasn.2021.3890.1054>
49. Codd R, Braich N, Liu J, Soe CZ, Pakchung AAH. Zn(II)-dependent histone deacetylase inhibitors: suberoylanilide hydroxamic acid and trichostatin A. Int J Biochem Cell Biol. 2009;41(4):736–9. <https://doi.org/10.1016/j.biocel.2008.05.026> PMID: 18725319
50. Alzuet G, Casella L, Perotti A, Borrás J. Acetazolamide binding to zinc(II), cobalt(II) and copper(II) model complexes of carbonic anhydrase. J Chem Soc Dalt Trans. 1994;(16):2347–51. <https://doi.org/10.1039/dt9940002347>
51. Yamazaki R, Kusunoki N, Matsuzaki T, Hashimoto S, Kawai S. Aspirin and sodium salicylate inhibit proliferation and induce apoptosis in rheumatoid synovial cells. J Pharm Pharmacol. 2002;54(12):1675–9. <https://doi.org/10.1211/002235702261> PMID: 12542898
52. Bergin JCJ, Tan KK, Nelson AK, Amarandei C-A, Hubscher-Bruder V, Brandel J, et al. 1-Hydroxy-2(1H)-pyridinone-based chelators with potential catechol O-Methyl transferase inhibition and neurorescue dual action against Parkinson's disease. Molecules. 2022;27(9):2816. <https://doi.org/10.3390/molecules27092816> PMID: 35566171
53. Al-Akeedi M, Najdawi M, Al-Balas Q, Al-Qazzan MB, Telfah ST. Novel anthraquinone amide derivatives as potential glyoxalase-I inhibitors. J Med Life. 2024;17(1):87–98. <https://doi.org/10.25122/jml-2023-0257> PMID: 38737655
54. Al-Balas QA, Hassan MA, Al-Shar'i NA, El-Elimat T, Almaaytah AM. Computational and experimental exploration of the structure-activity relationships of flavonoids as potent glyoxalase-I inhibitors. Drug Dev Res. 2018;79(2):58–69. <https://doi.org/10.1002/ddr.21421> PMID: 29285772
55. Al-Balasa QA, Hassana MA, Al Jabala GA, Al-Shar NA, Almaaytahb AM, El-Elimata T. Novel thiazole carboxylic acid derivatives possessing a “zinc binding feature” as potential human glyoxalase-I inhibitors. LDDD. 2017;14(11):1324–34. <https://doi.org/10.2174/1570180814666170306120954>
56. Al-Balas QA, Hassan MA, Al-Shar'i NA, Al Jabal GA, Almaaytah AM. Recent advances in glyoxalase-I inhibition. Mini Rev Med Chem. 2019;19(4):281–91. <https://doi.org/10.2174/1389557518666181009141231> PMID: 30306863
57. Al-Oudat BA, Jaradat HM, Al-Balas QA, Al-Shar'i NA, Bryant-Friedrich A, Bedi MF. Design, synthesis and biological evaluation of novel glyoxalase I inhibitors possessing diazenylbenzenesulfonamide moiety as potential anticancer agents. Bioorg Med Chem. 2020;28(16):115608. <https://doi.org/10.1016/j.bmc.2020.115608> PMID: 32690268
58. Audat SA, Al-Balas QA, Al-Oudat BA, Athamneh MJ, Bryant-Friedrich A. Design, synthesis and biological evaluation of 1,4-benzenesulfonamide derivatives as glyoxalase I inhibitors. Drug Des Devel Ther. 2022;16:873–85. <https://doi.org/10.2147/DDDT.S356621> PMID: 35378924
59. Kaur G, Dufour JM. Cell lines: valuable tools or useless artifacts. Spermatogenesis. 2012;2(1):1–5. <https://doi.org/10.4161/spmg.19885> PMID: 22553484
60. Vichai V, Kirtikara K. Sulforhodamine B colorimetric assay for cytotoxicity screening. Nat Protoc. 2006;1(3):1112–6. <https://doi.org/10.1038/nprot.2006.179> PMID: 17406391
61. Arabiyat S, Kasabri V, Al-Hiari Y, Bustanji YK, Albashti R, Almasri IM, et al. Antilipase and antiproliferative activities of novel fluoroquinolones and triazolo fluoroquinolones. Chem Biol Drug Des. 2017;90(6):1282–94. <https://doi.org/10.1111/cbdd.13049> PMID: 28639358
62. Arabiyat S, Kasabri V, Al-Hiari Y. Antilipolytic-antiproliferative activity of novel antidiabesity triazolo/fluoroquinolones. Jordan J Pharm Sci. 2020;13(1).
63. Kasabri V, Arabiyat S, Al-Hiari Y. Fluoroquinolones as a potentially novel class of antidiabesity and antiproliferative compounds: synthesis and docking studies. Can J Chem. 2020;98(10):635–45. <https://doi.org/10.1139/cjc-2020-016>
64. Al-Nuaimi A, Al-Hiari Y, Kasabri V, Haddadin R, Mamdooh N, Alalawi S, et al. A novel class of functionalized synthetic fluoroquinolones with dual antiproliferative - antimicrobial capacities. Asian Pac J Cancer Prev. 2021;22(4):1075–86. <https://doi.org/10.31557/APJCP.2021.22.4.1075> PMID: 33906299
65. Shkoor M, Tashtoush H, Al-Talib M, Mhaidat I, Al-Hiari Y, Kasabri V, et al. Synthesis and antiproliferative and antilipolytic activities of a series of 1,3- and 1,4-Bis[5-(R-sulfanyl)-1,2,4-triazol-3-yl]benzenes. Russ J Org Chem. 2021;57(7):1141–51. <https://doi.org/10.1134/s1070428021070149>
66. El-Hamoly T, El-Sharawy DM, El Refaye MS, Abd El-Rahman SS. L-thyroxine modifies nephrotoxicity by regulating the apoptotic pathway: the possible role of CD38/ADP-ribosyl cyclase-mediated calcium mobilization. PLoS One. 2017;12(9):e0184157. <https://doi.org/10.1371/journal.pone.0184157> PMID: 28892514
67. Pazzini V, D'Ambrosio M, Luceri C, Cinci L, Landucci E, Bilia AR, et al. Formulation of nanomicelles to improve the solubility and the oral absorption of silymarin. Molecules. 2019;24(9):1688. <https://doi.org/10.3390/molecules24091688> PMID: 31052197
68. Hoffmann H-H, Kunz A, Simon VA, Palese P, Shaw ML. Broad-spectrum antiviral that interferes with de novo pyrimidine biosynthesis. Proc Natl Acad Sci U S A. 2011;108(14):5777–82. <https://doi.org/10.1073/pnas.1101143108> PMID: 21436031

69. Arabiyat S, Kasabri V, Al-Hiari Y, Al-Masri I, Alalawi S, Bustanji Y. Dual glycation-inflammation modulation, DPP-IV and pancreatic lipase inhibitory potentials and antiproliferative activity of novel fluoroquinolones. *Asian Pac J Cancer Prev.* 2019;20(8):2503–14. <https://doi.org/10.31557/APJCP.2019.20.8.2503> PMID: 31450926
70. Al-Hiari Y, Arabiyat S, Kasabri V, Hamdan I, Almasri I, Yasin M, et al. Metal chelators as anticancer approach: Part I; novel 7-anisidine derivatives with multidentate at 7-8 carbons of fluoroquinolone scaffold as potential chelator anticancer and antilipolytic candidates. *Jordan J Pharm Sci.* 2023;16(2):402–25. <https://doi.org/10.35516/jjps.v16i2.1467>
71. Ibrahim R, Kasabri V, Sunoqrot S, Shalabi D, Alkhateeb R, Alhiari Y. Preparation and characterization of rutin-encapsulated polymeric micelles and studies of synergism with bioactive benzoic acids and triazolofluoroquinolones as anticancer nanomedicines. *Asian Pac J Cancer Prev.* 2023;24(3):977–89. <https://doi.org/10.31557/APJCP.2023.24.3.977> PMID: 36974553
72. Shamsheer R, Sunoqrot S, Kasabri V, Shalabi D, Alkhateeb R, Alhiari Y, et al. Preparation and characterization of capsaicin encapsulated polymeric micelles and studies of synergism with nicotinic acids as potential anticancer nanomedicines. *J Pharm Bioallied Sci.* 2023;15(3):107–25. https://doi.org/10.4103/jpbs.jpbs_311_22 PMID: 37705853
73. Mokhtar Z, Ali A, Awad S, Al-Qazzan M, Mahmoud M. Preparation of new Schiff base derivatives from chitosan grafted with polyvinylpyrrolidone and study of their antimicrobial activity. *Trop J Pharm Res.* 2025;24(7):935–48. <https://doi.org/10.4314/tjpr.v24i7.10>
74. Nakajima M, Yokoi T. MicroRNA: regulation of P450 and pharmacogenetics. In: *Handbook of pharmacogenomics and stratified medicine*. Elsevier; 2014. p. 385–401. <https://doi.org/10.1016/b978-0-12-386882-4.00019-0>
75. Yadav S, Sharma A, Nayik GA. Review of shikonin and derivatives: isolation, chemistry, biosynthesis, pharmacology and toxicology. *Front Pharmacol.* 2022;13:1–38. <https://doi.org/10.3389/fphar.2022.905755>
76. Lv X, Wang X-X, Hou J, Fang Z-Z, Wu J-J, Cao Y-F, et al. Comparison of the inhibitory effects of tolcapone and entacapone against human UDP-glucuronosyltransferases. *Toxicol Appl Pharmacol.* 2016;301:42–9. <https://doi.org/10.1016/j.taap.2016.04.009> PMID: 27089846
77. Hsu F-S, Wu J-T, Lin J-Y, Yang S-P, Kuo K-L, Lin W-C, et al. Histone deacetylase inhibitor, trichostatin A, synergistically enhances paclitaxel-induced cytotoxicity in urothelial carcinoma cells by suppressing the ERK pathway. *Int J Mol Sci.* 2019;20(5):1162. <https://doi.org/10.3390/ijms20051162> PMID: 30866433
78. Pieretti S, Saviano A, Mollica A, Stefanucci A, Aloisi AM, Nicoletti M. Calceolarioside A, a phenylpropanoid glycoside from *Calceolaria* spp., displays antinociceptive and anti-inflammatory properties. *Molecules.* 2022;27(7):2183. <https://doi.org/10.3390/molecules27072183> PMID: 35408584
79. Mukherjee Chatterjee S, Jain CK, Singha S, Das P, Roychoudhury S, Majumder HK, et al. Activity of coii-quinalizarin: a novel analogue of anthracycline-based anticancer agents targets human DNA topoisomerase, whereas quinalizarin itself acts via formation of semiquinone on acute lymphoblastic leukemia MOLT-4 and HCT 116 cells. *ACS Omega.* 2018;3(8):10255–66. <https://doi.org/10.1021/acsomega.8b00706> PMID: 31459155
80. Wang Y, Shang XY, Wang SJ. Structures, biogenesis, and biological activities of pyrano [4, 3-c] isochromen-4-one derivatives from the fungus *Phellinus igniarius*. *J Nat Prod.* 2007;70(2):296–9. <https://doi.org/10.1021/np060476h>
81. Hwang BS, Lee I-K, Choi HJ, Yun B-S. Anti-influenza activities of polyphenols from the medicinal mushroom *Phellinus baumii*. *Bioorg Med Chem Lett.* 2015;25(16):3256–60. <https://doi.org/10.1016/j.bmcl.2015.05.081> PMID: 26077494
82. Park I-H, Chung S-K, Lee K-B, Yoo Y-C, Kim S-K, Kim G-S, et al. An antioxidant hispidin from the mycelial cultures of *Phellinus linteus*. *Arch Pharm Res.* 2004;27(6):615–8. <https://doi.org/10.1007/BF02980159> PMID: 15283462
83. Shao HJ, Jeong JB, Kim K-J, Lee S-H. Anti-inflammatory activity of mushroom-derived hispidin through blocking of NF-κB activation. *J Sci Food Agric.* 2015;95(12):2482–6. <https://doi.org/10.1002/jsfa.6978> PMID: 25355452
84. Hassan KH, Al-hussani HA, Ibraim Oraibi A, Bashar Al-Qazzan M, Zainee HY, Al-Jashamy K, et al. Thermodynamic and kinetic assessment of cobalt II adsorption using green synthesized NiO/γ-Al2O3 nanoparticles. *Salud, Cienc Tecnol - Ser Conf.* 2025;4:1167. <https://doi.org/10.56294/sctconf20251167>
85. Lim J-H, Lee Y-M, Park SR, Kim DH, Lim BO. Anticancer activity of hispidin via reactive oxygen species-mediated apoptosis in colon cancer cells. *Anticancer Res.* 2014;34(8):4087–93. PMID: 25075033
86. Tamrakar S, Fukami K, Parajuli GP, Shimizu K. Antiallergic activity of the wild mushrooms of Nepal and the pure compound hispidin. *J Med Food.* 2019;22(2):225–7. <https://doi.org/10.1089/jmf.2018.4267> PMID: 30596532
87. Al-Balas QA, Al-Sha'er MA, Hassan MA, Al Zou'bi E. Identification of the first “Two Digit Nano-molar” inhibitors of the human glyoxalase-I enzyme as potential anticancer agents. *Med Chem.* 2022;18(4):473–83. <https://doi.org/10.2174/1573406417666210714170403> PMID: 34264188
88. Al-Shari'i NA, Al-Rousan EK, Fakhouri LI, Al-Balas QA, Hassan MA. Discovery of a nanomolar glyoxalase-I inhibitor using integrated ligand-based pharmacophore modeling and molecular docking. *Med Chem Res.* 2019;29(3):356–76. <https://doi.org/10.1007/s00044-019-02486-3>
89. Barua H, Bhagat N, Toraskar (mrs.) MP. Study of binding interactions of human carbonic anhydrase XII. *Int J Curr Pharm Sci.* 2016;9(1):118. <https://doi.org/10.22159/ijcpr.2017v9i1.16633>
90. Cheng Y, Wang L, Zhang S, Jian W, Zeng B, Liang L, et al. The investigation of NfkB inhibitors to block cell proliferation in OSCC cells lines. *Curr Med Chem.* 2024. <https://doi.org/10.2174/0109298673309489240>
91. Li R, Luo P, Guo Y, He Y, Wang C. Clinical features, treatment, and prognosis of SGLT2 inhibitors induced acute pancreatitis. *Expert Opin Drug Saf.* 2024;4:1–5. <https://doi.org/10.1080/14740338.2024.2396387> PMID: 39172128

92. Kang L, Gao X-H, Liu H-R, Men X, Wu H-N, Cui P-W, et al. Structure–activity relationship investigation of coumarin–chalcone hybrids with diverse side-chains as acetylcholinesterase and butyrylcholinesterase inhibitors. *Mol Divers.* 2018;22(4):893–906. <https://doi.org/10.1007/s11030-018-9839-y>

93. Shi S, Li K, Peng J, Li J, Luo L, Liu M, et al. Chemical characterization of extracts of leaves of *Kadsua coccinea* (Lem.) A.C. Sm. by UHPLC-Q-Exactive Orbitrap Mass spectrometry and assessment of their antioxidant and anti-inflammatory activities. *Biomed Pharmacother.* 2022;149:112828. <https://doi.org/10.1016/j.bipha.2022.112828>

94. Zhou J, Guo Z, Peng X, Wu B, Meng Q, Lu X, et al. Chrysotoxine regulates ferroptosis and the PI3K/AKT/mTOR pathway to prevent cervical cancer. *J Ethnopharmacol.* 2025;338(Pt 3):119126. <https://doi.org/10.1016/j.jep.2024.119126> PMID: 39557107

95. Lodi RS, Dong X, Wang X, Han Y, Liang X, Peng C, et al. Current research on the medical importance of *Trametes* species. *Fung Biol Rev.* 2025;51:100413. <https://doi.org/10.1016/j.fbr.2025.100413>

96. Guo Y, Han Z, Zhang J, Lu Y, Li C, Liu G. Development of a high-speed and ultrasensitive UV/Vis-CM for detecting total triterpenes in traditional Chinese medicine and its application. *Heliyon.* 2024;10(11):e32239. <https://doi.org/10.1016/j.heliyon.2024.e32239> PMID: 38882362

97. Wan H, Zhou S, Li C, Zhou H, Wan H, Yang J, et al. Ant colony algorithm-enabled back propagation neural network and response surface methodology based ultrasonic optimization of safflower seed alkaloid extraction and antioxidant. *Industr Crops Prod.* 2024;220:119191. <https://doi.org/10.1016/j.indcrop.2024.119191>

98. Chen Y, Fang L, Li G, Zhang J, Li C, Ma M, et al. Synergistic inhibition of colon cancer growth by the combination of methylglyoxal and silencing of glyoxalase I mediated by the STAT1 pathway. *Oncotarget.* 2017;8(33):54838–57. <https://doi.org/10.18632/oncotarget.18601> PMID: 28903386

99. Sharif M, Irfan M, Kousar K, Mamurova A, Duarte-Peña L, Hernández-Parra H, et al. Unlocking the biological potential of methyl antcinate A: a new frontier in cancer and inflammation application. *Naunyn Schmiedebergs Arch Pharmacol.* 2025;398(5):4727–45. <https://doi.org/10.1007/s00210-024-03544-3> PMID: 39630281

100. Xie Z, Zhao M, Yan C, Kong W, Lan F, Narengaowa, et al. Cathepsin B in programmed cell death machinery: mechanisms of execution and regulatory pathways. *Cell Death Dis.* 2023;14(4):255. <https://doi.org/10.1038/s41419-023-05786-0> PMID: 37031185

101. Bulatova NR, Kasabri NVN, Albsoul AM, Halaseh L, Suyagh M. Correlation of plasma and salivary osteocalcin levels with nascent metabolic syndrome components with and without pre/diabetes biochemical parameters. *Pharm Pract.* 2024;22(1):2880. <https://doi.org/10.18549/PharmPract.2024.1.2880>

102. Huang H, Zhang Y, Xu X, Liu Y, Zhao J, Ma L, et al. Design and synthesis of dual cathepsin L and S inhibitors and antimetastatic activity evaluation in pancreatic cancer cells. *Bioorg Med Chem Lett.* 2023;80:129087. <https://doi.org/10.1016/j.bmcl.2022.129087> PMID: 36427655

103. Citarella A, Petrella S, Moi D, Dimasi A, Braga T, Ruberto L, et al. Synthesis of α -fluorocinnamate derivatives as novel cathepsin S inhibitors with in vitro antiproliferative activity against pancreatic cancer cells. *Bioorg Med Chem.* 2024;115:117987. <https://doi.org/10.1016/j.bmc.2024.117987> PMID: 39509759

104. Waniczek D, Świętochowska E, Śnieta M, Kiczmer P, Lorenc Z, Muc-Wierzgoń M. Salivary concentrations of chemerin, α -defensin 1, and TNF- α as potential biomarkers in the early diagnosis of colorectal cancer. *Metabolites.* 2022;12(8):704. <https://doi.org/10.3390/metabo12080704> PMID: 36005576

105. Jin Y-Z, Xin Y-B, Li Y, Chen X-Y, Man D-A, Tian Y-S. Synthesis and selective anticancer activity evaluation of 2-phenylacrylonitrile derivatives as tubulin inhibitors. *Curr Med Chem.* 2024;31(15):2090–106. <https://doi.org/10.2174/0109298673263854231009063053> PMID: 38384112

106. Shin S, Sung BJ, Cho YS, Kim HJ, Ha NC, Hwang JI, et al. An anti-apoptotic protein human survivin is a direct inhibitor of caspase-3 and -7. *Biochemistry.* 2001;40(4):1117–23. <https://doi.org/10.1021/bi001603q> PMID: 11170436

107. Jazayeri MH, Aghaie T, Nedaeinia R, Manian M, Nickho H. Rapid noninvasive detection of bladder cancer using survivin antibody-conjugated gold nanoparticles (GNPs) based on localized surface plasmon resonance (LSPR). *Cancer Immunol Immunother.* 2020;69(9):1833–40. <https://doi.org/10.1007/s00262-020-02559-y> PMID: 32350593

108. El-Awady E-SE, Moustafa YM, Abo-Elmatty DM, Radwan A. Cisplatin-induced cardiotoxicity: mechanisms and cardioprotective strategies. *Eur J Pharmacol.* 2011;650(1):335–41. <https://doi.org/10.1016/j.ejphar.2010.09.085> PMID: 21034734

109. Ghosh A, Chénier I, Leung YH, Oppong AK, Peyot M-L, Madiraju SRM, et al. Adipocyte Angptl8 deletion improves glucose and energy metabolism and obesity associated inflammation in mice. *iScience.* 2024;27(12):111292. <https://doi.org/10.1016/j.isci.2024.111292> PMID: 39640567

110. Yang Y, Liu Y, Wang Y, Chao Y, Zhang J, Jia Y, et al. Regulation of SIRT1 and its roles in inflammation. *Front Immunol.* 2022;13:831168. <https://doi.org/10.3389/fimmu.2022.831168> PMID: 35359990